ACOUSTIC BARRIER OPTIMIZATION USING THE TOPOLOGICAL DERIVATIVE AND THE BOUNDARY ELEMENTH METHOD.

Agustín E. Sisamón[a], **Silja C. Beck**[b], **Adrián P. Cisilino**[a] **and Sabine Langer**[b]

[a]*INTEMA, Universidad Nacional de Mar del Plata – CONICET, Av. Juan B. Justo 4302, 7600 Mar del Plata, Argentina, cisilino@fi.mdp.edu.ar, http:// www.intema.gov.ar*

[b]*Institut für Angewandte Mechanik, Technische Universität Braunschweig, Spielmannstr. 11, 38106 Braunschweig, Germany, infaminfo@tu-bs.de, http:// www.infam.bau.tu-bs.de*

Keywords: Topological Derivative, Optimization, 2D Acoustic.

Abstract. Today, reduction of sound emission plays a vital role while designing objects of any kind. Desirable aspects might include decreased radiation in certain directions of such an object. This work shows an approach to compute the shape of an obstacle which fulfills best to prescribed design variables using the framework provided by the Topological Derivative and the Boundary Element Method (BEM).

The devised optimization tool takes advantage of the inherent characteristics of BEM to effectively solve the forward and adjoint acoustic problems arising from the Topological Derivative formulation, to deal with infinite and semi-infinite domains, plane and point waves, and to automatically adapt the model discretization to the evolving model topology.

The objective of the optimization is to achieve a prescribed sound pressure over a given region of the design domain. The design domain can be initially empty or it can contain an initial barrier to optimize. The Topological Derivative determines the places where new scatters need to be place in order to get close to the prescribed pressure. The capabilities of the proposed tools are demonstrated by solving a number of examples.

1 INTRODUCTION

Apart from functionality, the aspects of comfort have become increasingly important for users of almost any kind of product. As a result, today design processes take into account the acoustic properties of an object, i.e. its acoustic radiation. Especially for the case of objects acting as sound barrier it is desirable to minimize the radiation in certain directions.

The classical problem in acoustic design consists in finding the optimum geometric configuration of an object (say a sound barrier) to satisfy a given design objective for its radiation performance. A usual approach to tackle this problem is by means of shape optimization tools which consist in finding the optimal geometry within a class of domains having the same topology as the initial design, i.e., no holes are introduced in the optimization domain (Divo, 2003; Feijoo, Oberai, & Pinsky, 2004). However, the most general approach is topological optimization tools, which allow not only changing the shape of the object but its topology via the creation of internal holes. Topological optimization tools are capable to deliver optimal designs with a priori poor information on the optimal shape of the body.

Among the available topology optimization tools (see for example (Bendsøe & Sigmund, 2002)) the topological derivative is used in this work as its outcome can be easily adopted to the problem of acoustic scattering. The topological derivative was firstly introduced by (Cea, Gioan, & Michel, 1974) by combining a fixed point method with the natural extension of the classical shape gradient. The basic idea behind the topological derivative is the evaluation of cost function sensitivity to the creation of a hole. In this way, wherever this sensitivity is low enough (or high enough depending on the nature of the problem) the material can be progressively eliminated. This concept was mathematically introduce for shape optimization by (Sokolowski & Zochowski, 1999). More recently, (Novotny, Feijóo, Taroco, & Padra, 2003) introduced a novel procedure for the computation of the topological derivative for potential elasticity problems. That approach was implemented within the Boundary Element Method (BEM) framework for two dimensional potential problems by (Cisilino, 2006), and for two and three dimensional elasticity problems by (Carretero Neches & Cisilino, 2008) and (Bertsch, Cisilino, Langer, & Reese, 2008) respectively.

With respect to acoustic wave propagation, (Feijoo, 2004) proposed a method for imaging 'hidden' sound-hard objects via inverse scattering analysis using the topological derivative approach. In this case the cost function is the difference between a prescribed scattering pattern and the one measured when illuminating the hidden object by a planar wave travelling in a given direction. Starting from an empty optimization domain, the topological derivative indicates the positions where to place rigid inclusions to produce a scattered field which will converge to the prescribed one. More recently, (Carpio & Rapún, 2008) extended the method due to (Feijoo, 2004) in order to allow the solution of problems with initial scatters in the optimization domain and to deal with sound-soft objects.

In this work, the topological derivative as proposed by (Feijoo, 2004) and extended by (Carpio & Rapún, 2008) is implemented within a BEM framework. The devised optimization tool takes advantage of the inherent characteristics of the direct BEM formulation for acoustics in the frequency domain to effectively solve the forward and adjoint acoustic problems arising from the Topological Derivative formulation. The versatility of this method is tested solving several application examples in infinite or semi-infinite medium and different type of incident waves.

2 THE FORWARD AND INVERSE SCATTERING PROBLEM

We assume a certain medium where a number of scatters interact with an incident radiation

with a particular type of wave (electromagnetic, acoustic, etc.). The incident wave interacts with the objects and the medium, the reflection is measure at a certain receptors place far enough from the scatters. If the incident and measured wavefields are known it might be possible to find the scatters. This is the way that many detecting device works, i.e. radar, sonar, etc.

The strategy used in this work for solving this identification problems follows the one proposed by (Feijoo, 2004) where the concept of Topological Derivative is applied to identification problems in the field of acoustic scattering. This section will introduce the concepts of forward and inverse problems which are needed for the computation of the Topological Derivative
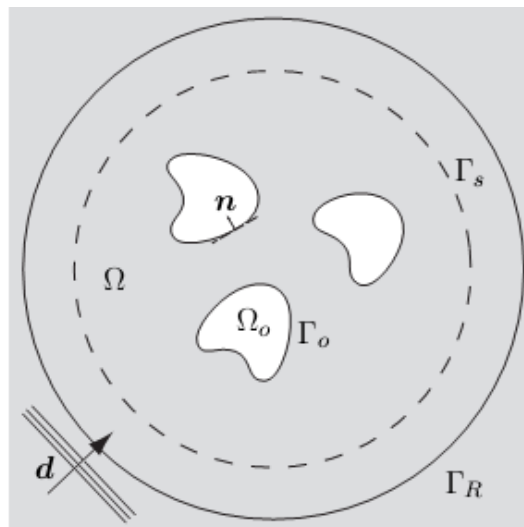

Figure 1: The inverse scattering problem.

2.1 The Forward Problem

Following (Feijoo, 2004), the setting of the problem is depicted in Figure 1, where Ω is a homogeneous infinite medium with one or more sound hard scatters Ω_0 with boundary Γ_0. Notice that in Figure 1 the boundary Γ_s, where the receptors are place, is assumed to be a circle of radius R_s that encloses all the scatters. In the formulation presented in this work this is not mandatory, in fact it could be used to solve more realistic problems where Γ_s is an arrangement of discrete points. The total wavefield is given by the addition of the incident and scattered fields, this is $p=p_{inc}+p_s$. This acoustic scattering problem is governed by Helmholtz partial differential equation:

$$\nabla^2 p(x) + \kappa^2 p(x) = 0 \;\; in \; \Omega = \mathbb{R} \backslash \Omega_0 \tag{1}$$

$$\nabla p(x) \cdot n = 0 \quad on \; \Gamma_0 \tag{2}$$

$$\lim_{r \to \infty} \sqrt{r} \left(\frac{\partial p_s}{\partial n} - i\kappa p_s \right) = 0 \tag{3}$$

where the incident waves, planar or point are given respectively by Eq. (4) and Eq. (5).

$$p_{inc}(\mathbf{x}, \mathbf{d}) = e^{i\kappa\mathbf{x}\cdot\mathbf{d}} \tag{4}$$

$$p_{inc}(\mathbf{x}, \mathbf{x_0}) = -\frac{i}{4}H_0^{(1)}(\kappa r) \quad with \, r := |\mathbf{x} - \mathbf{x_0}| \tag{5}$$

where $H_0^{(1)}(\kappa r)$ is the Hankel function of the first kind and order zero, $\mathbf{d}$ is the propagation direction of the planar wave, $\kappa = \omega/c$ the wave number (the relation of the angular frequency ω to the speed of sound c) and $\mathbf{x_0}$ is the point source location. Eq (2) is the sound hard boundary condition and Eq (3) is the Sommerfeld radiation condition on the propagation of the scattered field p_s, which implies that only outgoing waves are allowed at infinity.

The forward problem is solving Eq. (1)-(3) when p_{inc} and the scatters Ω_0 are known. If the total field p on the set of receptors Γ_s (these measured values will be denoted as p_m) is known but not all or none of the scatters are known we now need to solve an inverse problem.

2.2 The Inverse Problem

The inverse problem consist in finding the shape of the scatters Ω_0 such that the solution of the forward problem Eq (1)-(3) equals the measured values p_m, this is $p|\Gamma_s=p_m$. This condition is enforced via a least-squares-type minimization problem of the form: find $\hat{\Omega}$ such that

$$\hat{\Omega} = \arg \, min \, J(\Omega) \tag{6}$$

where

$$J(\Omega) = \frac{1}{2}\int_{\Gamma_s} |p - p_m|^2 d\Gamma \tag{7}$$

with p being the solution of the forward problem Eq (1)-(3).

The inverse problem can be written as an optimization problem with Ω being the design variable and the forward problem, Eq (1)-(3), as constrain on the scalar field p. Thus, the solution of this problem is given by a domain that minimizes Eq. (7). When several measurements corresponding to different directions $\mathbf{d_j}$ for the incident wave are available, the inverse problem can be extended to consider all of them:

$$J(\Omega) = \frac{1}{2}\sum_{j=1}^{N}\int_{\Gamma_s} |p^j - p_m^j|^2 d\Gamma \tag{8}$$

with p^j the solution of N forward problems so now there are N constrains.

Remarks

Notice that this section presents the forward and inverse acoustic scattering problems for infinite regions, this formulation can be easily extend for solving in semi-infinite regions. Consider that the domain Ω limited by an infinite rigid plane (Γ_H). Since the plane is rigid ($\nabla p(x) \cdot n = 0$), total reflection occurs for any incident wave at Γ_H. The incident wave equation (Eq. (4) and Eq. (5)) are therefore

$$p_{inc}(\mathbf{x}, \mathbf{d}) = e^{i\kappa\mathbf{x}\cdot\mathbf{d}} + e^{i\kappa\mathbf{x}\cdot\mathbf{d'}} \tag{9}$$

$$p_{inc}(\mathbf{x}, \mathbf{x_0}) = -\frac{i}{4}\left[H_0^{(1)}(\kappa r) + H_0^{(1)}(\kappa r_2)\right] \quad with \begin{array}{l} r := |\mathbf{x} - \mathbf{x_0}| \\ r_2 := |\mathbf{x} - \mathbf{x_0'}| \end{array} \tag{10}$$

where $\mathbf{d'}$ and $\mathbf{x_0'}$ are the images of $\mathbf{d}$ and $\mathbf{x_0}$ with respect to Γ_H (see Figure 2)

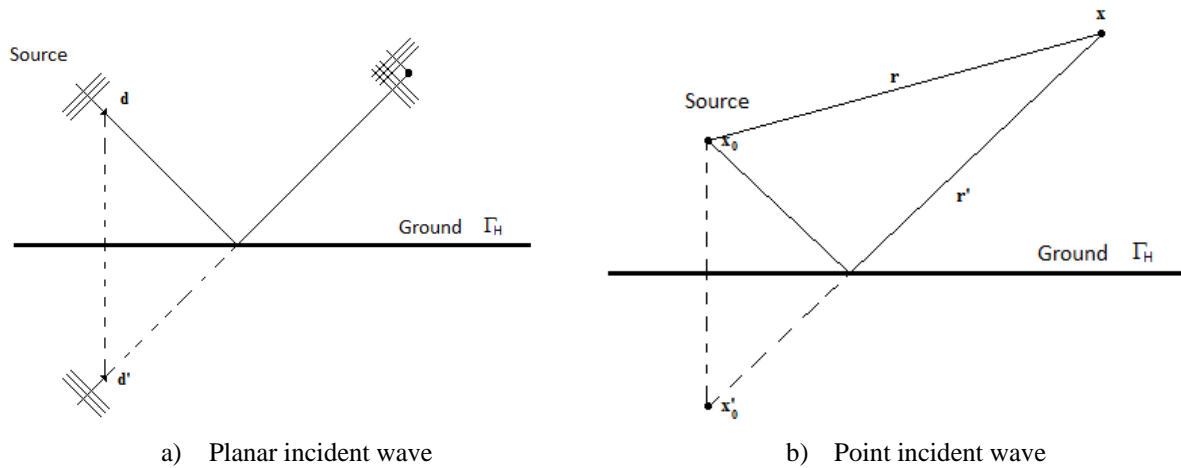a)   Planar incident wave   b)   Point incident wave

Figure 2 Incident wave reflection of a two-dimensional half-space Ω limited by an infinite plane Γ_H.

3   THE TOPOLOGICAL DERIVATIVE

The strategy to solve the inverse problem starts with an initial domain Ω then, the functional in Eq. (6) is changed to account for the modification of the domain by introducing a small circular hole, $B_\varepsilon(\mathbf{x})$, centered at $\mathbf{x}$ and of radius ε. The new domain is denoted by $\Omega_\varepsilon = \Omega \backslash B_\varepsilon(\mathbf{x})$ (see Figure 3).

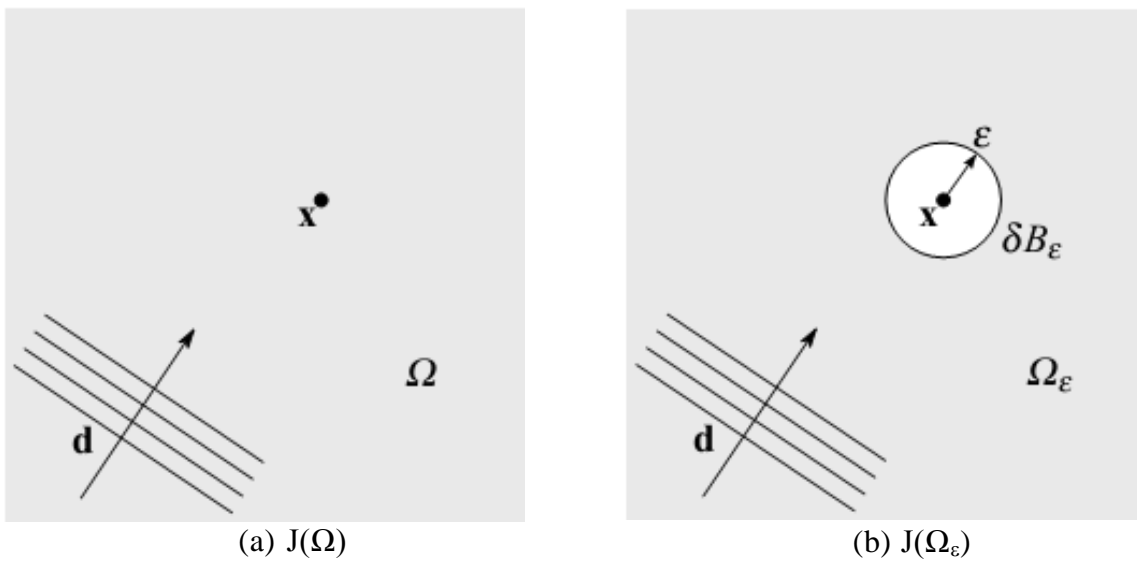(a) J(Ω)   (b) J(Ω_ε)

Figure 3 Strategy for the solution of the inverse problem

Denoting by $f(\varepsilon)$ the negative value of the 'size' of the hole B_ε, the asymptotic expansion of the functional in Eq. (6) can be stated as follows.

$$J(\Omega_\varepsilon) = J(\Omega) + f(\varepsilon)D_T(x) + \mathcal{O}(f(\varepsilon)) \tag{11}$$

where $D_T(\mathbf{x})$ is the topological derivative which measures the rate of change of the functional value with respect to the size of the scatterer $B_\varepsilon(\mathbf{x})$, or in a more illustrative way as the size of the small scatterer goes to zero, it measures the sensitivity of a shape functional when an infinitesimal 'hole' is subtracted from the domain. Then the remaining term $\mathcal{O}(f(\varepsilon))$ satisfies

$$\lim_{\varepsilon \to 0^+} \frac{\mathcal{O}(f(\varepsilon))}{f(\varepsilon)} = 0 \tag{12}$$

The scalar field $D_T(\mathbf{x})$ can be constructed by moving the point $\mathbf{x}$ in $\mathbb{R}^2$. Then the identification technique can be motivated as follows: if it is necessary to choose where many small scatterers are to be placed in order to minimize the value of $J(\Omega)$ (and as a consequence recreate the shape of the scatterer by obtaining the scattering pattern that is close to p_m), they should be placed where D_T attains the lowest values. Then the topological derivative is expressed by the following limit:

$$D_T(\mathbf{x}) = \lim_{\varepsilon \to 0^+} \frac{J(\Omega_\varepsilon) - J(\Omega)}{f(\varepsilon)} \tag{13}$$

where $f(\varepsilon)$ is a monotonically decreasing negative function such that $\lim_{\varepsilon \to 0^+} f(\varepsilon) = 0$. The selection of $f(\varepsilon)$, which corresponds to the size of the 'hole' but not necessarily is its measure in $\mathbb{R}^2$, is a non-trivial. The $f(\varepsilon)$ depends on the boundary condition specified on the surface δB_ε of the scatterer and it must satisfy $0 < |D_T(\mathbf{x})| < \infty$.

The direct application and implementation of the concept in Eq. (13) is not straightforward, as it is not possible to establish a homeomorphism between domains with different topologies (domains with and without the hole).

Many authors, and in particular (Feijoo, 2004) for the case of acoustic problems, proposed an alternative definition of the $D_T(\mathbf{x})$ that overcomes the above difficulties. They propose assimilating the creation of a hole to the perturbation of a preexisting hole whose radius tends to zero (see Figure 4). Therefore, both topologies of the optimization domain are now similar and it is possible to establish a homeomorphism between them. According to this new definition, the expression for the $D_T(\mathbf{x})$ is

$$D_T(\mathbf{x}) = \lim_{\substack{\varepsilon \to 0^+ \\ \delta\varepsilon \to 0}} \frac{J(\Omega_{\varepsilon+\delta\varepsilon}) - J(\Omega_\varepsilon)}{f(\varepsilon + \delta\varepsilon) - f(\varepsilon)} \tag{14}$$

where $J(\Omega_\varepsilon)$ and $J(\Omega_{\varepsilon+\delta\varepsilon})$ are the cost functions evaluated for the reference and perturbed domain, ε is the initial radius of the hole, δ_ε is a small perturbation of the hole radius and f is a regularization function. The function f is problem dependent and $f(\varepsilon) \to 0$ when $\varepsilon \to 0$.

(a) $J(\Omega_\varepsilon)$ (b) $J(\Omega_{\varepsilon+\delta\varepsilon})$
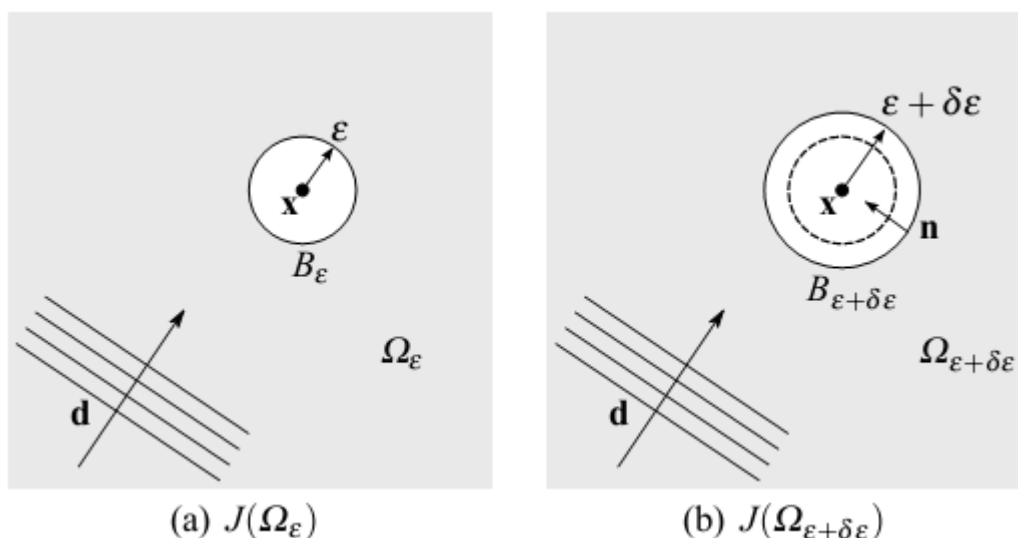
Figure 4 Definition of the topological derivative using the shape sensitivity analysis approach

It could be argued that the new definition of the $D_T(\mathbf{x})$ in Eq. (14) merely provides the sensitivity of the problem when the size of the hole is perturbed and not when it is effectively created (as it is the case in the original definition of the topological derivative). However, it is understood that to expand a hole of radius ε, when $\varepsilon\rightarrow 0$, is nothing more than creating it (a complete mathematical proof that establishes the relation between both definitions of the D_T is given in (Novotny et al., 2003)). Moreover, the relationship between the two definitions constitutes the formal relation between the $D_T(\mathbf{x})$ and the shape sensitivity analysis. The advantage of the novel definition for the topological derivative given by Eq. (14) is that the whole mathematical framework developed for the shape sensitivity analysis can now be used to compute the $D_T(\mathbf{x})$.

Among the available shape sensitivity analysis results, the differentiation of the shape derivative for acoustic problems presented by (Feijoo, 2004) is of particular interest here. Given a shape functional $J(\Omega)$, the shape derivative $DJ(\Omega)\cdot V$ in the direction given by the vector field $V(\mathbf{x})$ is defined as follows:

$$DJ(\Omega) \cdot V = \frac{d}{d\varepsilon}J(\phi_\varepsilon(\Omega))|_{\varepsilon=0} \tag{15}$$

where φ_ε is the mapping $\varphi_\varepsilon(\mathbf{x})=x+\varepsilon V(\mathbf{x})$ between the reference and perturbed domains. The computation of the shape derivative in Eq. (15) for the functional $J(\Omega)$ in Eq. (6) for the case in which the direction $V(\mathbf{x})$ is that of the normal vector $n(\mathbf{x})$ (see Figure 4) results in (a detailed derivation of this result is in (Feijoo et al., 2004)):

$$DJ(\mathbf{x}) \cdot V = \Re\left[\int_{\Gamma_S} (\nabla\bar{\lambda} \cdot \nabla p - \kappa^2\bar{\lambda}p)v_n d\Gamma\right] \tag{16}$$

where the operator $\Re$ is the real part of the complex solution of the integral, $v_n = V.n$ is the normal component of the vector V, p is the solution of the forward problem in Eq. (1)-(3) and λ is the solution of the an adjoint variational problem (the overbar symbol indicating the conjugate complex). It can be demonstrated mathematically (for further details see (Feijoo, 2004)) that this adjoint problem is equivalent to the following boundary-value problem:

$$\nabla^2\lambda(\mathbf{x}) + \kappa^2\lambda(\mathbf{x}) = (p_m(\mathbf{x}) - p(\mathbf{x}))\delta_{\Gamma_S} \quad in \ \Omega = \mathbb{R}\backslash\Omega_0 \tag{17}$$

$$\nabla\lambda(\mathbf{x}) \cdot n = 0 \quad on \ \Gamma_0 \tag{18}$$

$$\lim_{r\to\infty} \sqrt{r}\left(\frac{\partial\lambda}{\partial n} + i\kappa\lambda\right) = 0 \tag{19}$$

In Eq. (17), $\delta\Gamma_s$ is the Dirac delta-function defined on the sampling surface Γ_s. It should be noted that the adjoint field λ corresponds to the backpropagation (note the plus sign in Eq. (19) and compare with Eq. (3)) of the mismatch between the solution given by the forward model and the measured signature at Γ_s.

The topological derivative can be computed now by combining the results in Eq. (14) and Eq. (16). Having in mind that the boundary condition on ∂B_ε is the one of a rigid object (see Eq. (2)), it results

$$D_T(\mathbf{x}) = -\lim_{\varepsilon\to 0^+}\frac{1}{f'(\varepsilon)}\Re\left[\int_{\partial B_\varepsilon} (\nabla\bar{\lambda}_\varepsilon \cdot \nabla p_\varepsilon - \kappa^2\bar{\lambda}_\varepsilon p_\varepsilon)v_n d\partial B_\varepsilon\right] \tag{20}$$

where p_ε and λ_ε are solutions of the forward and adjoint problems posed in the configuration $\Omega_\varepsilon=\Omega\backslash B_\varepsilon(\mathbf{x})$. An asymptotic analysis of these solutions and their gradients at ∂B_ε reveals that

these terms are of $\mathcal{O}(1)$ as $\varepsilon \rightarrow 0$ (see Feijoo (2004)). Therefore, to satisfy $0 < |D_T(\mathbf{x})| < \infty$ it is required that $f'(\varepsilon) = -2\pi\varepsilon$, which implies that $f(\varepsilon) = -\pi\varepsilon^2$. The final expression for the topological derivative is then

$$D_T(\mathbf{x}) = \Re\left[2\nabla\bar{\lambda}_\varepsilon(\mathbf{x}) \cdot \nabla p_\varepsilon(\mathbf{x}) - \kappa^2\bar{\lambda}_\varepsilon(\mathbf{x})p_\varepsilon(\mathbf{x})\right] \tag{21}$$

where p and λ are solutions of the forward and adjoint problems. Eq (21) holds regardless of the structure of the incident wave. It may be a plane wave Eq. (4) or point source Eq. (5).

4   COMPUTATION OF THE TOPOLOGICAL DERIVATIVE

The computation of the $D_T(\mathbf{x})$ requires of the solution of the forward and adjoint problems. The idea is to compute the $D_T(\mathbf{x})$ on a grid of points, the areas where the Topological Derivative attains the lowest (more negatives) values indicate the possible location of scatters. The boundary Γ_0 would be consider as a finite set of receptors ($\mathbf{x_k}$, k=1,...,M). In this discretized scheme the inverse problem (Eq. (8)) with one incident wave becomes, minimize:

$$J(\Omega) = \frac{1}{2}\sum_{k=1}^{M}\left|p^j - p_m^j\right|^2 \tag{22}$$

If more than one incident wave are present on the problem, the total $D_T(\mathbf{x})$ field is simple the algebraic sum of the $D_T(\mathbf{x})$ for each incident wave.

4.1 Computation of the adjoint and forward problems with no scatters

This section will set the focus on problems where there is no previous information about the location and the number of scatters. If we assume no obstacles on an infinite domain $\Omega = \mathbb{R}^2$ and M receptors over Γ_s then the solution to the forward problem p is simply the incident wave given by Eq. (4)-(5), and the adjoint problem $\bar{\lambda}$ is:

$$\begin{cases} \nabla^2\bar{\lambda}(\mathbf{x}) + \kappa^2\bar{\lambda}(\mathbf{x}) = \sum_{k=1}^{M}\overline{\left(p_m(\mathbf{x_k}) - p(\mathbf{x_k})\right)}\delta_{\Gamma_S} & in\ \Omega \\[2em] \lim_{r \to \infty}\sqrt{r}\left(\frac{\partial\bar{\lambda}}{\partial n} - i\kappa\bar{\lambda}\right) = 0 \end{cases} \tag{23}$$

Following the strategy proposed by (Carpio & Rapún, 2008) for the computation of the adjoint problem an explicit formula for $\bar{\lambda}$ is obtained using the outgoing fundamental solution of the Helmholtz equation (Eq. (1)). This fundamental solution p^* corresponds to the field generated by a unit concentrated harmonic source located on $\mathbf{x_k}$, Eq. (5) which satisfy the Sommerfeld radiation condition at infinity and $\nabla^2 p^*(\mathbf{x}, \mathbf{x_k}) + \kappa^2 p^*(\mathbf{x}, \mathbf{x_k}) = -\delta(\mathbf{x} - \mathbf{x_k})$. Then the solution of the adjoint problem is:

$$\bar{\lambda}(\mathbf{x}) = \sum_{k=1}^{M}\overline{\left(p_m(\mathbf{x_k}) - p(\mathbf{x_k})\right)}p^*(\mathbf{x}, \mathbf{x}_k), \qquad in\ \Omega \tag{24}$$

Now the Topological Derivative of the cost functional can be computed for an empty domain by Eq. (21).

4.2 Computation of the adjoint and forward problems with initial scatters

Consider now that there is some information on the scatters presents on $\Omega = \mathbb{R}^2$, for example the shape or location of one scatter. The forward problem solves Eq. (1)-(3), this has to be done by numerical method. The adjoint problem is given through Eq. (17)-(19) or can be write in a more convenient way as

$$
\begin{cases}
\nabla^2 \bar{\lambda}(\mathbf{x}) + \kappa^2 \bar{\lambda}(\mathbf{x}) = \sum_{k=1}^{M} \overline{(p_m(\mathbf{x_k}) - p(\mathbf{x_k}))} \delta_{\Gamma_S} & in \ \Omega = \mathbb{R}\backslash\Omega_0 \\
\nabla \bar{\lambda}(\mathbf{x}) \cdot n = 0 & on \ \Gamma_0 \\
\lim_{r \to \infty} \sqrt{r} \left(\frac{\partial \bar{\lambda}}{\partial n} - i\kappa\bar{\lambda} \right) = 0 &
\end{cases}
\tag{25}
$$

This problem can be decomposed into $\bar{\lambda} = \lambda_i + \lambda_s$ where λ_i is the solution of the adjoint problem on an empty domain Eq. (24) and λ_s

$$
\begin{cases}
\nabla^2 \lambda_s(\mathbf{x}) + \kappa^2 \lambda_s(\mathbf{x}) = 0 & in \ \Omega = \mathbb{R}\backslash\Omega_0 \\
\nabla \lambda_s(\mathbf{x}) \cdot n = \nabla \lambda_i(\mathbf{x}) \cdot n & on \ \Gamma_0 \\
\lim_{r \to \infty} \sqrt{r} \left(\frac{\partial \lambda_s}{\partial n} - i\kappa\lambda_s \right) = 0 &
\end{cases}
\tag{26}
$$

Notice that Eq. (26) and Eq. (1)-(3) are completely analogous. The only difference is on the right hand sides. Therefore, to compute numerically the adjoint problem one just needs to follow the same steps for computing the forward problem.

4.3 Direct BEM formulation for acoustic scattering

Several numerical methods can be implemented to solve the forward and adjoint problem, e.g. techniques based in series expansions, finite elements, method of moments, etc. This section explains how to use the direct BEM formulation (Wrobel & Aliabadi, 2002) in the frequency domain for the computation of both, forward and adjoint problems. To apply the BEM for a certain problem two prerequisites have to be fulfilled: the domain needs to be homogeneous and the fundamental solution known. The boundary integral equation (BIE) is derived by applying the method of weighted residuals to Eq. (1), using the fundamental solution as test function, applying Green's second identity and the filter function of the Dirac delta function. Then, moving the source point ξ to the boundary leads to the BIE:

$$
c(\xi)p(\xi) + \int_\Gamma p_s(\mathbf{x})q^*(\mathbf{x}, \xi)d\Gamma_{\mathbf{x}} = \int_\Gamma q_s(\mathbf{x})p^*(\mathbf{x}, \xi)d\Gamma_{\mathbf{x}} + p_{inc}(\xi)
\tag{27}
$$

the term $p_{inc}(\xi)$ is the incident wave or waves (Eq. (4) for planar sources and Eq. (5) for point sources) at the point ξ.

As was defined previously, the fundamental solution p^* describes the reactions in an unbounded domain caused by a point source with the intensity of 1 at point ξ. The fundamental solution needs to fulfill the inhomogeneous differential equation

$$
\nabla^2 p^*(\mathbf{x}, \xi) + \kappa^2 p^*(\mathbf{x}, \xi) = -\delta(\mathbf{x} - \xi)
\tag{28}
$$

with $\delta(\mathbf{x}-\xi)$ being the Dirac delta function.

The fundamental solution p^* as defined previously and its derivative $\partial p^*/\partial n = q^*$ (denoting the sound flux) are given in 2D for infinite domain by

$$p^*(\mathbf{x}, \xi) = -\frac{i}{4} H_0^{(1)}(\kappa r) \quad with \; r := |\mathbf{x} - \xi| \tag{29}$$

$$q^*(\mathbf{x}, \xi) = \frac{i\kappa}{4} H_1^{(1)}(\kappa r) \frac{\partial r}{\partial n} \tag{30}$$

As an exact solution of the BIE is generally not available the boundary is discretized into a finite number of linear boundary elements, as depicted in Figure 6(left)). The values for acoustic pressure p and flux q are approximated using shape functions in the form of $p=\mathbf{n}p$ and $q=\mathbf{n}q$, respectively. The vector $\mathbf{n}$ holds the shape functions while p and q contain the values of pressure and flux at the nodes. Setting up the BIE (Eq. (27)) for each node (collocation method) leads to a system of equations

$$\mathbf{Gq_s} - \mathbf{Hp_s} = \mathbf{p_{inc}} \tag{31}$$

where the matrices $\mathbf{G}$ and $\mathbf{H}$ contain the results of the integrals for shape functions and the fundamental solutions p^* and q^* along the element domains. It is worth noting here that since the present application deals with sound-hard scatters only, the sound flux is always zero along the complete model boundary. Thus, the system in Eq. (31) reduces to

$$-\mathbf{Hp_s} = \mathbf{p_{inc}} \tag{32}$$

which is used to compute the sound pressure p on the model boundary. Further details about the boundary element formulation and implementation can be found in any classic BEM book, e.g. (Wrobel & Aliabadi, 2002).

Solving a forward problem in the BEM context gives in the first step the pressure field p over the surface of the scatterer. In a second step the values of $p(\mathbf{x})$ are computed for all internal points within the design domain using the internal counterpart of the BIE introduced in Eq. (27). Recalling that the scatterer is considered as sound-hard, for an incident wave $p_{inc}(\xi)$ (Eq. (4) or Eq. (5))

$$p(\xi) = \int_\Gamma -p_s(\mathbf{x}) q^*(\mathbf{x}, \xi) d\Gamma + p_{inc}(\xi) \quad \text{for } \xi \in \Omega \tag{33}$$

Similarly, the gradients $\nabla p(x)$ can be computed at the internal points using the space derivatives of Eq. (33) with respect to the internal points

$$\frac{\partial p(\xi)}{\partial x_i} = \int_\Gamma -p_s(\mathbf{x}) \frac{\partial q^*(\mathbf{x}, \xi)}{\partial x_i} d\Gamma + \frac{\partial p_{inc}(\xi)}{\partial x_i} \quad \text{for } \xi \in \Omega \tag{34}$$

Remarks

Notice that this section presents the direct BEM formulation for acoustic scattering on infinite regions. If BEM formulation for semi-infinite regions wants to be implemented, one needs to use

$$p^*(\mathbf{x}, \xi) = -\frac{i}{4} \left[H_0^{(1)}(\kappa r_1) + H_0^{(1)}(\kappa r_2) \right] \quad \text{with} \quad \begin{matrix} r_1 := |\mathbf{x} - \xi| \\ r_2 := |\mathbf{x} - \xi'| \end{matrix} \tag{35}$$

as fundamental solution instead of Eq. (29) and

$$q^*(\mathbf{x}, \xi) = \frac{i}{4} \left[H_1^{(1)}(\kappa r_1) \frac{\partial r_1}{\partial n} + H_1^{(1)}(\kappa r_2) \frac{\partial r_2}{\partial n} \right] \tag{36}$$

instead of Eq. (30). The second term of those equations corresponds to the reflected waves

due to the presences of the infinite rigid plane Γ_H. Where r_1 is the distance from the radiating surface and r_2 corresponds to the distance from the radiating point to ξ' (the image of ξ respect to Γ_H, see Figure 5 Two dimensional half-space limited by and infinite rigid plane Γ_H and interior boundaries Γ_0Figure 5).
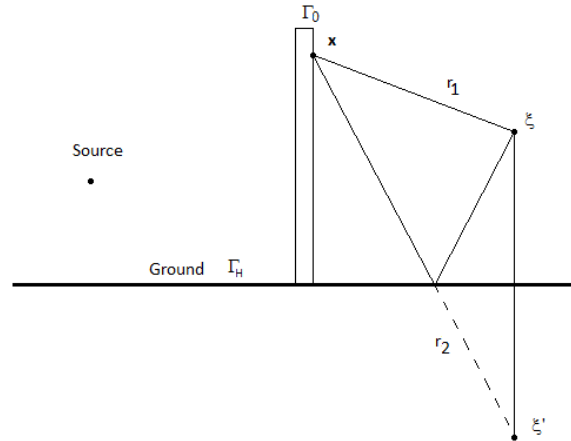

Figure 5 Two dimensional half-space limited by and infinite rigid plane Γ_H and interior boundaries Γ_0

5   IMPLEMENTATION

This work has presented an effective way to compute the D_T within the BEM framework for different kinds of incident waves and infinite or semi-infinite domain. This section shows the computational scheme implemented.

The implementation can be divided into four steps: setting up the BEM model, solving the forward problem, solving the adjoint problem and computation of the D_T.

5.1 Setting up the BEM model

The model discretization is key issue for the performance of the implemented algorithm. The initial BEM model is discretized using two-node linear elements and a regular array of internal points following the pattern depicted in Figure 6. The size of the elements on the boundary needs to be at least 7-8 times smaller than the wave length.
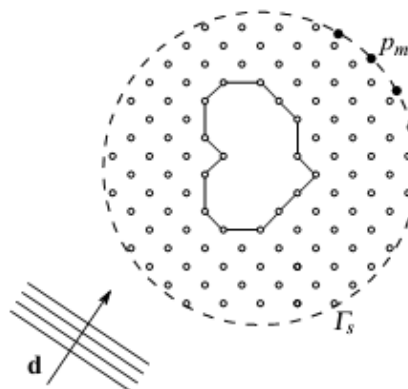

Figure 6 Internal points pattern.

The internal points are distributed on the design domain using a regular array. In the same way as the elements the distance between internal points needs to have the same ratio with the wave length if a good resolution on D_T is required.

5.2 Solving Forward Problem

Solving the forward problem with a BEM formulation is straightforward.

Compute p_{inc}: The pressure and its derivatives are computed at the positions of the internal points, the receptors and the boundary nodes. This computation is than for all incoming wave using Eq (3), (4) if the problem is posed on infinite domain or Eq. (9) and (10) for semi-infinite domain.

Solve BEM problem (if initial boundary exists): The BEM system of equations is assembled following section 3.3 to obtain Eq. (32). This system is solved for each incoming wave.

Compute $p(x)$ and $\nabla p(x)$ for internal points and receptors (if initial boundary exists): Assemble and compute Eq. (33) and Eq. (34) for the selected type of region and for each incoming wave.

As the BEM matrices depend on geometrical parameters and wave number only, they need to be computed only once if the frequency of all sources is the same. Furthermore these matrices will be used for solving the adjoint problem later.

5.3 Solving the Adjoint Problem

As was shown in previous sections the adjoint problem can be computed as a forward problem with point sources located at the positions of the receptors.

Compute source amplitude: Compute the discrepancy (Eq. (24)) between p_m and p on the receptors for each incoming wave.

Solve the BEM problem: Solve the BEM model with point incoming waves located at the receptors and the amplitude given by the previously computed discrepancies. Notice that the solution of the adjoint problem for each incident wave involves the solution of as many forward problems as the number of receptors, M.

5.4 Computation of the DT

Once p, λ and their derivatives are known, the computation of DT is just applying Eq. (21) for each incoming wave and adding this results. This will lead to the final Topological Derivative field over the entire design domain. The shape of the unknown scatter will be given by the positions of the internal points with the most negative values of D_T

5.5 Implementation Notes

The procedure was implemented in Matlab taking advantage of the numerical and matrix capabilities of this language.

The inputs for this problem are:

- Type of region: Infinite or Semi-infinite
- Size of the design domain and distance between internal points.
- Coordinate and connectivity of the BEM mesh for the initial geometry (if exist an initial one)
- Number, data (frequency, amplitude, position or direction of propagation) and type (point or planar) of incident waves
- Coordinate values of receivers over Γ_S.
- Prescribed pressure over Γ_S for each source.

6   EXAMPLES

Results for three examples are presented in this section. In order to assess the performance of the implemented method, the first two are validation examples while the last one consists in an application problem.

6.1 Identification of scatters on an infinite domain

This first example consists in the identification of two hidden scatters, one circle of radius R = 0.5m centered on (1,1) and a square of size 0,5 centered on (-0.75,-0.75). In the first case the D_T is computed over an empty design domain. This optimization domain is a square of size 4m x 4m discretized using 40401 internal points which are placed on a square grid with a step l = 0.02m.

The objective values, p_m, along the virtual surface Γ_s is the scattered field for the scatters when it is illuminated by 50 planar sound waves (the angle of incidence equally distributed over 2π) with a wavenumber $\kappa = 29.73$ m^{-1} and an amplitude A = 1 Pa. The objective values are specified at N = 100 points evenly distributed along Γ_s. Figure 7 shows the set-up of the problem.
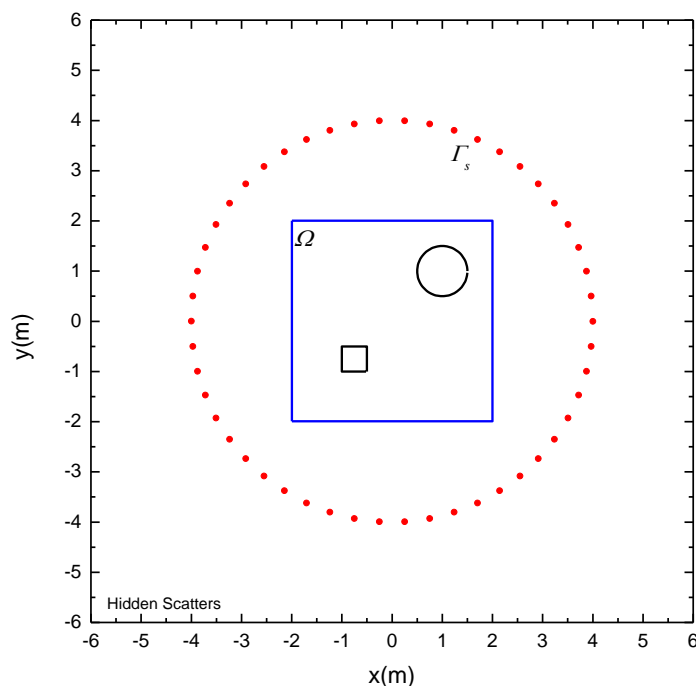

Figure 7 Problem set-up

The topological derivative is computed by adding up the solutions obtained for each incident wave. The D_T field is plotted in Figure 8 (a). It can be seen that the minimum values for the D_T are situated were the hidden scatters (marked with a black line) are.

The second case considers the square as an initial geometry, thus the only hidden scatter is the circle. The D_T field is shown in Figure 8 (b). In this case the boundary of the square is discretized in 100 linear elements of size l=0.02m for the BEM implementation.

(a) Empty Domain   (b) Initial Scatter
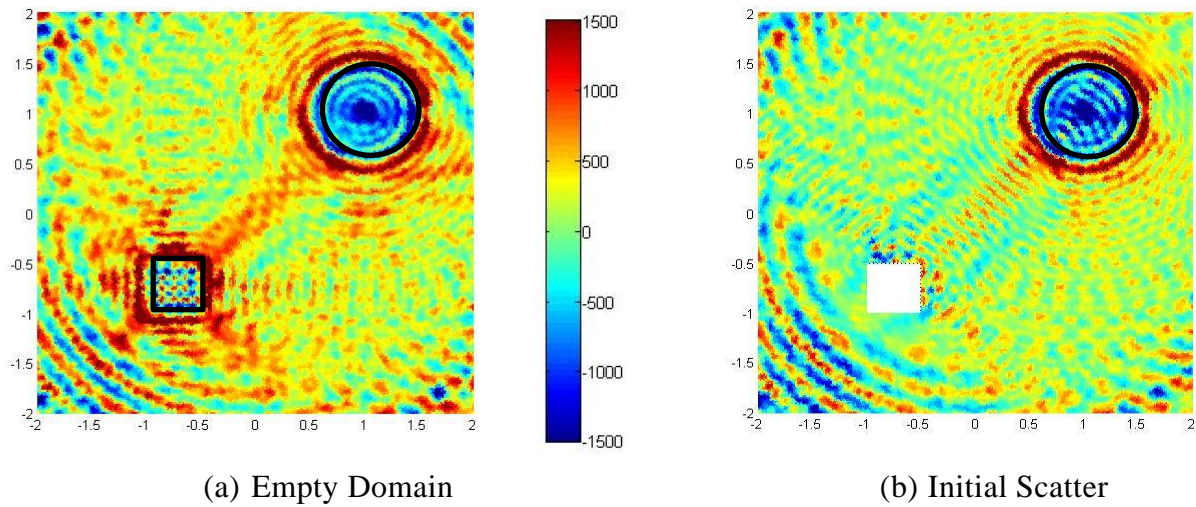
Figure 8 Topological Derivative field.

It can be seen that the Topological Derivative properly identifies the shape of the hidden scatters in both cases, starting on an empty domain or an initial scatter.

6.2 Identification of scatters on a semi-infinite domain

This example shows the capabilities of the implemented method for solving identification problems on semi-infinite domains. Following the same procedure of the previous example, the set-up of the problem is shown in Figure 9. The domain is a square of length 6m discretized on 14641 points which are placed on a square grid with a step l = 0.05m. The hidden scatter is a rectangle of 0,4m x 4m with its center located on (4m, 2m). The objective values, p_m, along the virtual surface Γ_s is the scattered field for the scatters when it is illuminated by 26 planar sound waves (the angle of incidence equally distributed from 0 to π) with a wavenumber $\kappa = 9.91$ m^{-1} and an amplitude A = 1 Pa. The objective values are specified at N = 100 points evenly distributed along Γ_s. Figure 9 shows the set-up of the problem. Figure 10 shows the Topological Derivative field for this problem.
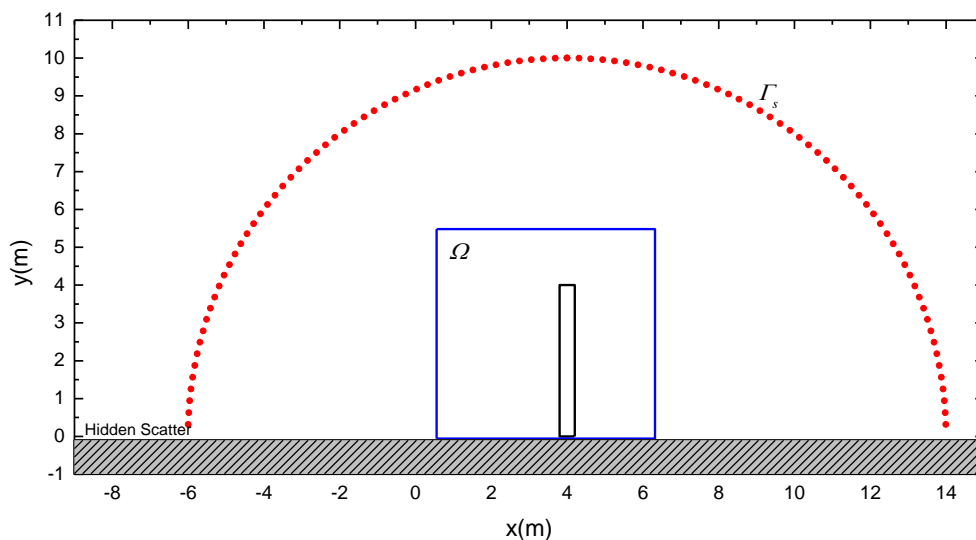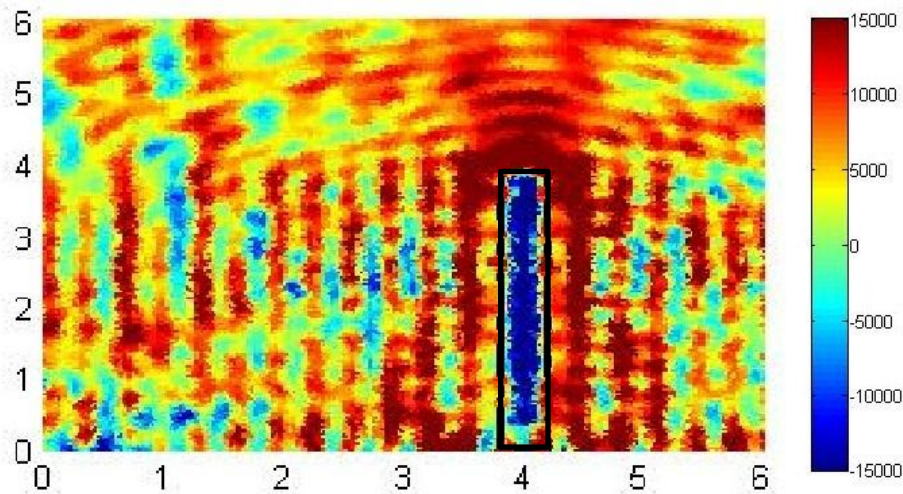

Figure 9 Problem set-up

Figure 10 Topological Derivative field.

In concordance with the previous example this one shows the identification of the hidden scatter using the D_T on semi-infinite domains

6.3 Application example: Optimization of a sound barrier

This example consists of the optimization of the geometry of a barrier depicted in Figure 11. The objective of the problem is to minimize the pressure (considering both the incident and the scattered fields) behind the barrier when it is illuminated by a single point source located at (15m, 0.5m). The initial geometry of the barrier is a rectangle with dimensions 0.25m x 4m and with its barycenter in the position (5m, 2m). The objective pressure is specified on a discrete arrange of 32 points (Γs) evenly distributed on a rectangle of size 5m x 2.5m with barycenter in (0.5m, 0.75).
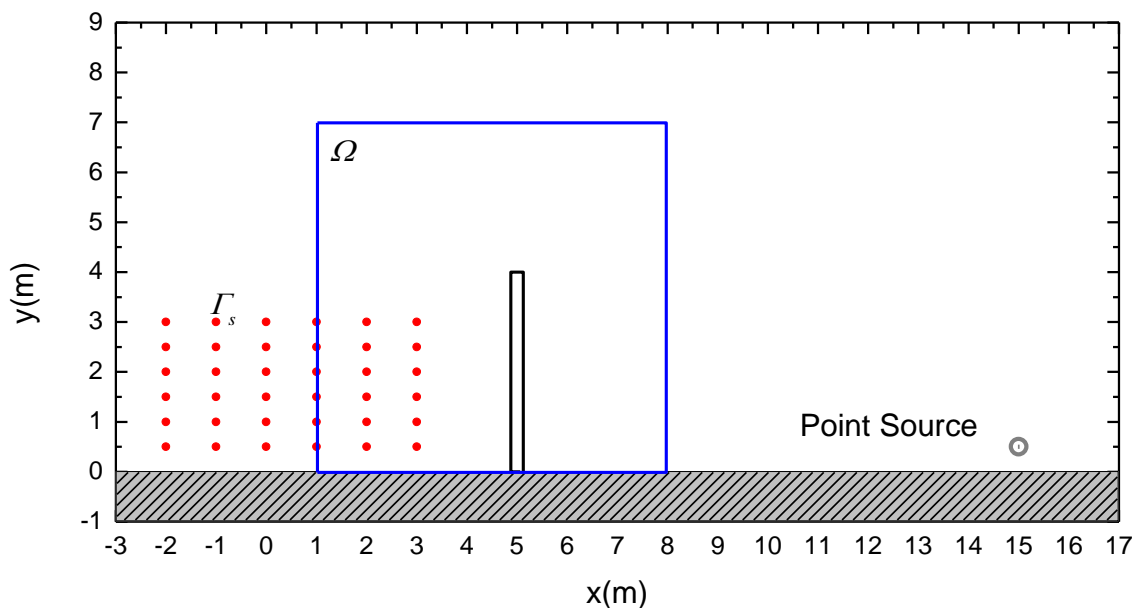

Figure 11 Problem set-up

The wavenumber of the incident wave is $\kappa = 9.9$ m^{-1} and its amplitude is A = 1 Pa. The

optimization domain (Ω) is a square of size 7m x 7m discretized using 12427 internal points placed on a square grid with a step 0.0625m. The initial geometry of the barrier is discretized using 164 elements.

(a) Sound Pressure Level field   (b) Topological Derivative field
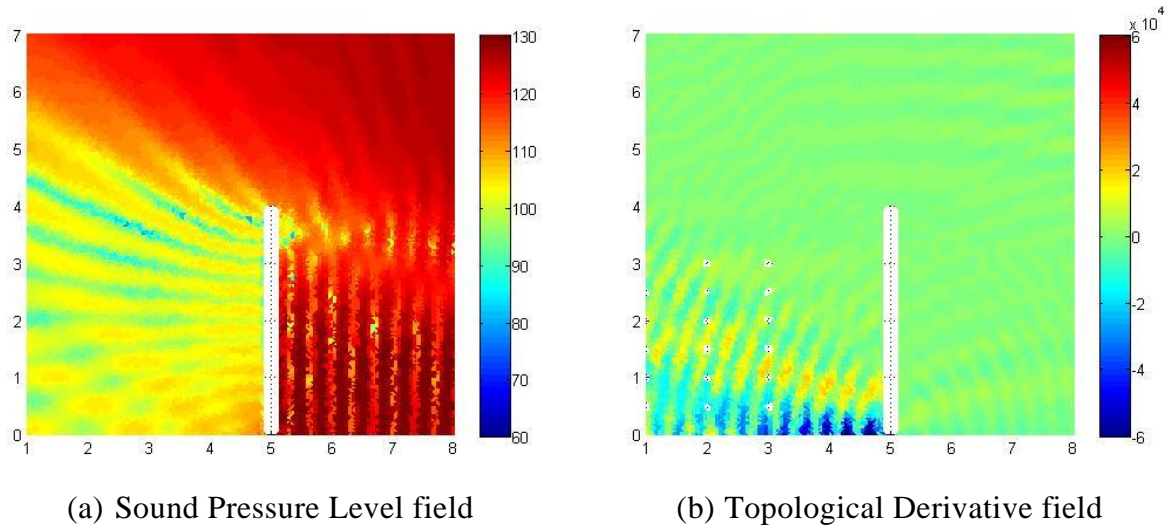
Figure 12 SPL and D_T fields for initial barrier.

Figure 12 shows the sound pressure level (SPL) and Topological Derivative fields of the barrier. The most negative values of D_T are on the left hand side of the barrier. Thus, in order to improve this barrier new scatters are placed on the positions with the 20 most negative values of D_T. The resulting barrier is analyzed to show the improvement, this result is depicted in Figure 13.
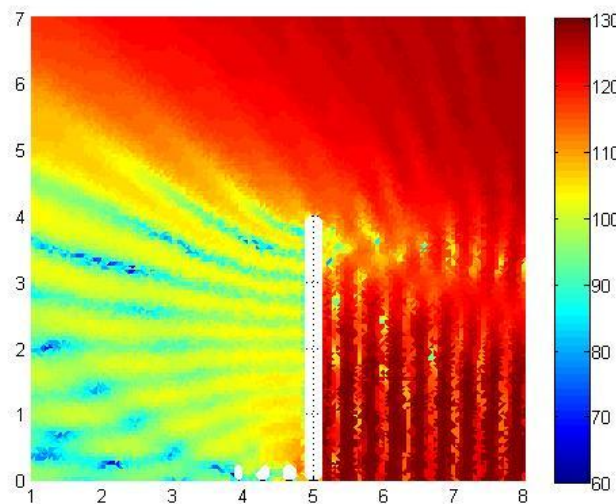

Figure 13 SPL field of the optimized barrier

In the case the left hand side of the barrier is not available for placing the scatterers the D_T field is forced to be equal to zero for all internal points where x<=5 and y<=4. Now the most negative values of D_T are on the right hand side of the barrier. Again, the new scatters are placed on the positions with the 20 most negative values of D_T. The penalized D_T field and SPL field for the resulting barrier are shown in Figure 14.
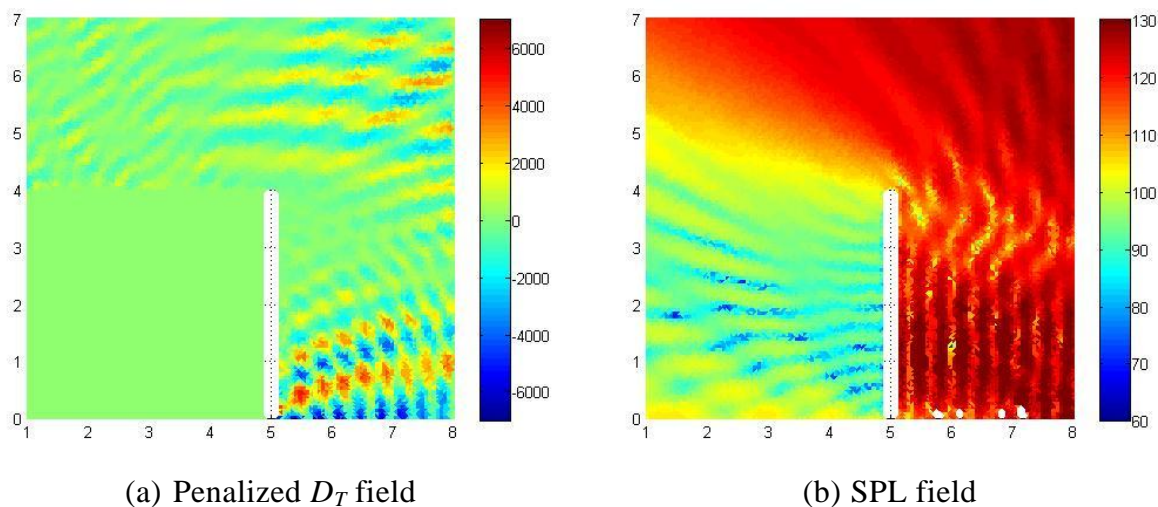
(a) Penalized D_T field   (b) SPL field

Figure 14 Optimized barrier with constrains.

Figure 15 shows a quantitative comparison between the SPL fields over Γs for the three cases, initial barrier, optimized barrier and constrained optimized barrier. The points on Γs are sorted in ascending order according to SPL values for the initial barrier. It can be seen in this figure that for the optimized barrier the SPL is effectively decreased at every position on Γs. On the other hand when the D_T is penalized the SPL decreases for approximately 75% of Γs. An overall comparison of the cost functional reported in Table 1 is consistent with these results.
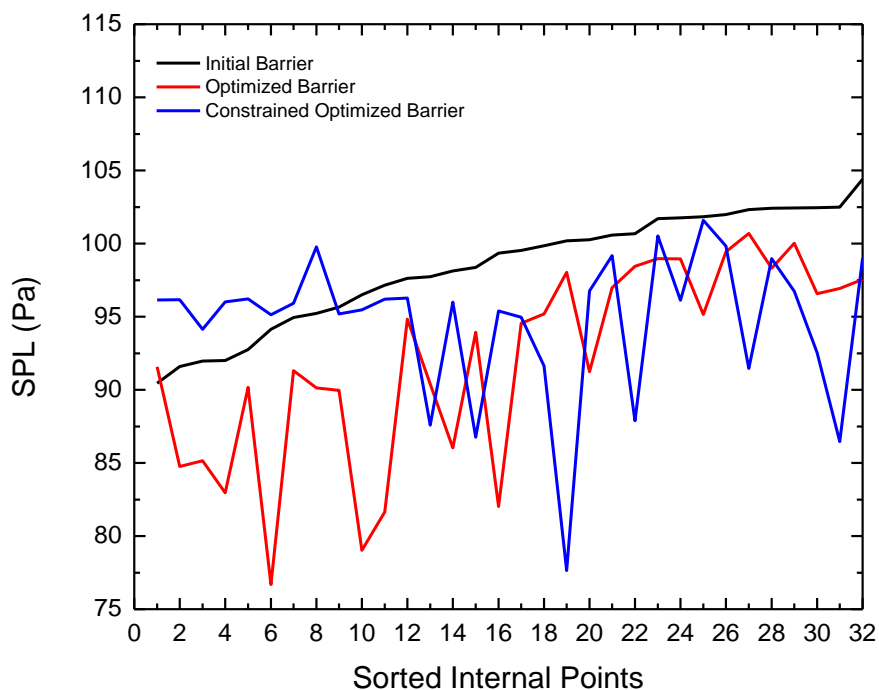

Figure 15 SPL field of the optimized barrier

	Cost functional
Initial Barrier	60.45436
Optimized Barrier	22.29711
Constrained Optimized Barrier	28.25805

Table 1 Comparison of the Cost Functional

7 CONCLUSION

It has been presented in this work a BEM implementation of the topological derivative for acoustic problem. The devised optimization tool takes advantage of the inherent characteristics of the direct BEM formulation for acoustics in the frequency domain to effectively solve the forward and adjoint acoustic problems necessary for the computation of the Topological Derivative. The proposed strategy can be used to deal with identification and optimization problems, starting from empty design domain and domains with initial scatters, infinite and semi-infinite domain and different kinds of sources. The versatility of this method is tested solving three application examples.

REFERENCES

Bendsøe, M. P., & Sigmund, O. (2002). *Topology Optimization* (p. 370). Springer.

Bertsch, C., Cisilino, A. P., Langer, S., & Reese, S. (2008). Topology Optimization of 3D Elastic Structures Using Boundary Elements. *PAMM - Proc. Appl. Math. Mech.*, *8*(1), 10771–10772. doi:10.1002/pamm.200810771

Carpio, A., & Rapún, M. L. (2008). Topological Derivatives for Shape Reconstruction. *INVERSE PROBLEMS AND IMAGING*, *1943/2008*, 85–133.

Carretero Neches, L., & Cisilino, A. P. (2008). Topology optimization of 2D elastic structures using boundary elements. *Engineering Analysis with Boundary Elements*, *32*(7), 533–544. doi:10.1016/j.enganabound.2007.10.003

Cea, J., Gioan, A., & Michel, J. (1974). Adaptation de la methode du gradient a un probleme d'identification de domaine. In R. Glowinski & J. Lions (Eds.), *Computing Methods in Applied Sciences and Engineering Part 2* (pp. 391–402). Springer Berlin / Heidelberg. doi:10.1007/3-540-06769-8_19

Cisilino, A. P. (2006). Topology Optimization of 2D Potential Problems Using Boundary Elements. *Comput Model Eng Sci*, *15*(2), 99–106.

Divo, E. (2003). Shape optimization of acoustic scattering bodies. *Engineering Analysis with Boundary Elements*, *27*(7), 695–703. doi:10.1016/S0955-7997(03)00022-5

Feijoo, G. R. (2004). A new method in inverse scattering based on the topological derivative. *Inverse Problems*, *20*(6), 1819–1840. doi:10.1088/0266-5611/20/6/008

Feijoo, G. R., Oberai, A. A., & Pinsky, P. M. (2004). An application of shape optimization in the solution of inverse acoustic scattering problems. *Inverse Problems*, *20*, 199–228. doi:10.1088/0266-5611/20/1/012

Novotny, A. ., Feijóo, R. a., Taroco, E., & Padra, C. (2003). Topological sensitivity analysis. *Computer Methods in Applied Mechanics and Engineering*, *192*(7-8), 803–829. doi:10.1016/S0045-7825(02)00599-6

Sokolowski, J., & Zochowski, A. (1999). On the Topological Derivative in Shape Optimization. *SIAM Journal on Control and Optimization*, *37*(4), 1251–1272. doi:10.1137/S0363012997323230

Wrobel, L. C., & Aliabadi, M. H. (2002). *The boundary element method: Applications in thermo-fluids and acoustics* (p. 468). John Wiley and Sons.